Superconducting array for high-field magnetic resonance imaging

J. Wosik,[a] L. Xue, L.-M. Xie, and M. R. Kamel
Texas Center for Superconductivity and Electrical and Engineering Department, The University of Houston, Houston, Texas 77204, USA

K. Nesteruk
Institute of Physics of The Polish Academy of Sciences, 02–668 Warsaw, Poland

James A. Bankson
Department of Diagnostic and Interventions, Health Science Center, The University of Texas, Houston, Texas USA

(Received 2 June 2007; accepted 2 October 2007; published online 30 October 2007)

We report on the design of a planar 200 MHz superconducting two-resonator array for magnetic resonance imaging (MRI) applications. The array was made out of a double-sided thin $YBa_2Cu_3O_{7-x}$ film on *r*-cut sapphire substrate and consists of two 24 mm diameter resonators with built-in planar capacitors for coupling to the tuning and matching electronics. Required for the performance of the MRI array, rf isolation of two resonators was accomplished by built-in planar capacitors, and the mechanism of resonator-to-resonator decoupling was analyzed. The signal-to-noise gain as a result of using high-T_c superconductor resonators/arrays was calculated and compared with experimental data. © *2007 American Institute of Physics*.
[DOI: 10.1063/1.2801384]

In magnetic resonance imaging (MRI), a sample (body) is placed in a dc magnetic field, a sequence of field gradient and rf excitation pulses are applied, and the relaxing nuclei (usually protons) produce weak decaying rf signals that are detected by a rf receiver probe.[1] There is a need for high resolution and/or fast scan imaging but the intrinsically weak signal-to-noise ratio (SNR) is the main limitation to achieving these goals. The noise in a MRI system is primarily thermal noise in the receiver Faraday coil (rf resonator) and in the body.[2] In the body-dominated noise regime, little advantage is gained by the reduction of conductive coil losses. However, either for low-field MRI (smaller than 0.5 T) or for small coil sizes at high-field MRI, when the coil noise is the governing source of noise, it has long been recognized that cooling the receiving coils[2] or using high-T_c (HTS) materials[3–5] reduce this noise contribution and therefore can significantly increase the SNR.[6]

For many years, the implementation of small cryogenic coils in MRI systems was not practical at high magnetic fields because of their small sizes resulting in a small field of view (FOV). This changed in 1990 (Ref. 7) after the introduction of arrays of electromagnetically isolated small-size coils designed to simultaneously acquire signals from all coils. Such concept has offered resolution and SNR of small receiving coils combined with FOV typical for large volume coils without increasing the imaging time. However, its realization was hindered by the lack of multichannel systems. It has changed recently when introduction of new array encoding techniques, in which reduction of image acquisition time,[8] became a subject of great interest.

HTS thin films are very attractive for the use as surface receiver coils because such films at 77 K exhibit an extremely low surface resistance R_s of the order of microhms at 100 MHz.[9] This resistance is several orders of magnitude lower than the R_s of copper at the same frequency and temperature. Implementation of HTS arrays is challenging because practical cryogenic coil array designs require capacitive coupling to each of the HTS elements, low-loss electronic tuning and matching, as well as coil-to-coil mutual inductance cancellation circuits.[10]

In order to fulfill these requirements, we have developed a HTS-based design of a multilayered planar structure (HTS/dielectric/metal), which, in addition to HTS resonators, includes built-in resonator capacitors for tuning, matching, and coil-to coil decoupling [Figs. 1(a) and 1(b)]. Each single-element coil consists of two split rings placed on opposite sides of the substrate and rotated versus each other by 180°.[11]

The 0.5 μm thick $YBa_2Cu_3O_{7-x}$ films[12] were deposited by evaporation on both sides of a single-crystal 0.43 mm *r*-cut sapphire substrate ($\varepsilon=10.2$) and were patterned according to a simulated array layout (Ansoft, Inc., HFSS software). Optical lithography and wet etching were used to pattern the array. Superconductor-electronic circuit coupling capacitors were fabricated by evaporating 0.2 and 0.5 μm dielectric CeO_2 and gold layers, respectively, on the upper side of the patterned YBCO films. Figure 1(a) shows an expanded view of the $Ag/CeO_2/YBCO$ and $Au/CeO_2-Al_2O_3/YBCO$ ca-

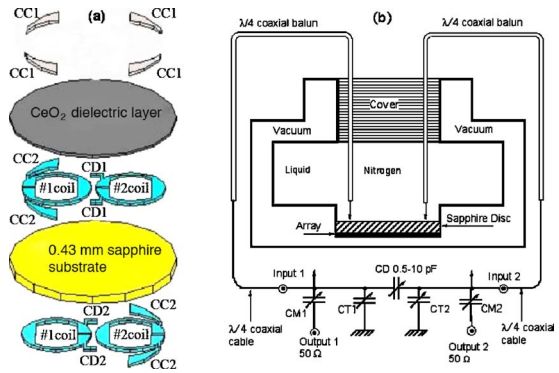

FIG. 1. (Color online) (a) Expanded view of the multilayered design. (b) CC1, CC2 and CD1, CD2 depict coupling-to-electronics and coil-to-coil decoupling capacitor plates, respectively. (b) A sketch of the G-10 cryostat with the circuit of CM, CT, and CD capacitors for matching, tuning, and coil-to-coil decoupling.

[a]Electronic mail: jarek@uh.edu

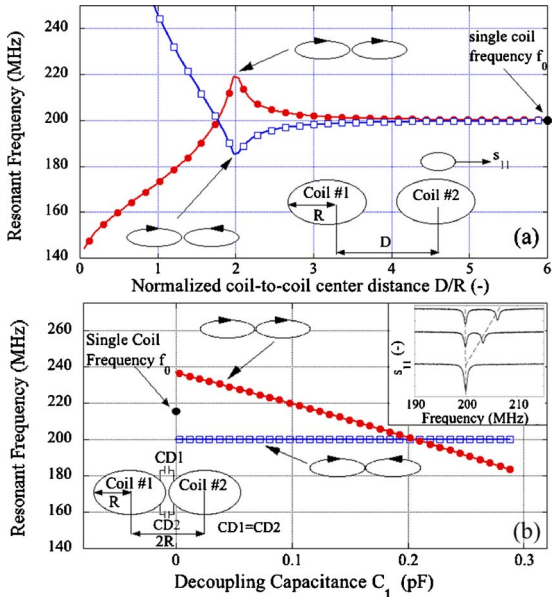

FIG. 2. (Color online) (a) Plot illustrating rf decoupling for a two-element array by geometrical overlapping. Resonance frequency of each mode (rf currents in and out phases) was calculated vs coil center distance D (changing from "fully overlapping" to "fully apart" positions). (b) Calculated frequencies of two modes vs decoupling capacitance for the array of two coils placed next to each other are plotted. Inset shows a measured reflection coefficient s_{11} from coil 1.

pacitors. A matching, tuning, and detuning circuitry cable was soldered to the upper gold plates of the coupling capacitors, CC1 [Fig. 1(a)].

Each array element was tuned to 216 MHz and matched to a 50 Ω preamplifier, using a tuning and matching circuit [Fig. 1(b)]. The coils were electromagnetically decoupled (isolated) from each other by two planar capacitors, CD1 and CD2 ($YBCO/Al_2O_3/YBCO$), built-in between the coils; fine decoupling adjustment was provided by an external CD capacitor. The array was detuned from the transmit coil during transmit pulse. It was placed in a custom-made G-10 77 K cryostat and was separated from boiling nitrogen with a 5-mm-thick sapphire window [Fig. 1(b)].

Placing two coils close to each other results in coupling between them and causes splitting of mode's frequency and a significant reduction of SNR in the array. Such a coupling can be described by mutual inductance M_{12} between coils 1 and 2 due to the magnetic flux (in conjunction with a magnetic vector potential A_1) produced by the first coil with a current I_1 that interacts with the second coil,

$$M_{1,2} = \frac{-1}{I_1} \oint \mathbf{A}_1(r_2) \cdot d\mathbf{r}_2. \tag{1}$$

A system of two coupled coils has two stable resonant modes: the first one when rf currents flow in the same direction (even mode) in both coils and the second one when rf currents flow in the opposite directions (odd mode). Frequency order of these modes depends on the sign of their mutual inductance,

$$f_{\mp} = \frac{1}{2\pi} \sqrt{\frac{1}{(L \pm |M_{12}|)C}}, \tag{2}$$

where L is the inductance and C is the capacitance of the resonator. Calculations of the frequency for both modes vs distance between coils' centers are shown in Fig. 2(a).

One of the standard methods used to decouple MRI coils is to adjust overlapping adjacent elements until mutual inductance is canceled. For a HTS array, coil overlapping for decoupling is not practical because it requires nonplanar HTS films deposition technology. We will use this concept only for simulations of SNR versus number of array elements. To electromagnetically isolate HTS coils we choose capacitive decoupling using built-in decoupling capacitors[13] marked as CD1 and CD2 in Figs. 1(a) and 2(b).

We have noticed that for such decoupling is only the even mode is influenced by the decoupling capacitance [Fig. 2(b)]. In the odd mode, due to the same voltage, there is no rf current in the CD capacitors while in the even mode, when the currents in the coils are in phase, the rf current flows in the capacitor. Therefore, by changing the CD capacitance, decoupling is achieved by making the higher mode's frequency equal to that of the lower mode. At the decoupled point, there is no resonance in coil 2, while all the energy is stored in coil 1. For capacitive decoupling the decoupled frequency is equal to the lower mutual inductance split frequency, thus each array element has to be designed to resonate at 216 MHz. This is in contrast to the geometrical decoupling case when each single element of the array has to be designed for 200 MHz. The decoupling of two coils was verified experimentally by acquiring images (not shown here) when only one channel (1 or 2) of the Bruker 4.7 T scanner was on. For both the cases, an image from only one coil was seen while the other coil was clearly not excited. The s_{12} transmit signal coefficient between the coils was −28 dB.

In order to show the relationship between the SNR, the number of the array coils, and the attainable SNR gain while using cryogenic coils, we have calculated the relative array SNR versus the number of individual coils in the array. The calculations were done for copper and HTS (25×50 mm^2 overall dimension) arrays cooled to 77 K and were normalized to SNR 295 Cu array. Body size was assumed to be a cylinder with 25 mm diameter. We followed the quasistatic approach, and SNR was calculated in standard way[14] as

$$\mathrm{SNR} = G \frac{\omega B_t(\mathbf{r})}{\sqrt{R_{\mathrm{tot}}}}, \tag{3}$$

where $G = M_0(B_0)\nu/(4k_B T_{\mathrm{RT}} \Delta f)^{0.5}$, ν is a voxel volume and M_0 the magnetization density, proportional to the applied dc magnetic field B_0. T_{RT} is room temperature and Δf is the bandwidth. In Eq. (3), ω is the Larmor frequency at B_0. Calculations of the array SNR require an image reconstruction algorithm to combine the complex individual coil images (small individual FOV) into a single composite image with full FOV. A set of weighting coefficients α_i for each coil was derived in order to obtain an optimal combination of coils's signal and noise needed for such reconstruction. $B_t(r)$ is the weighted sum of the transverse magnetic field $b_{t,i}(r)$ at a given location r for each coil in the array and can be expressed as

$$B_t(\mathbf{r}) = \sum_{i=1}^{N} \alpha_i b_{t,i}(\mathbf{r}) = \boldsymbol{\alpha}^T \cdot \mathbf{b}_t. \tag{4}$$

The noise voltage induced in the coil is a sum of voltage noise due to Ohmic losses of the coil itself and due to body loading of the coil (eddy currents losses). The effective total thermal noise resistance matrix R_{tot}, can be expressed as

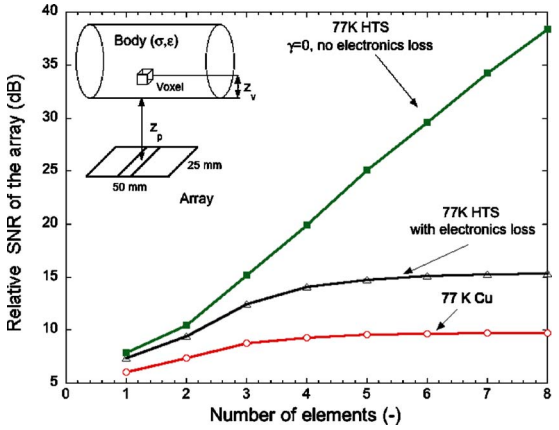

FIG. 3. (Color online) Calculations of the SNR vs the number of elements of the linear 25×50 mm^2 array for 77 K Cu and HTS (with and without losses due to the electronics). The SNR is normalized to the SNR of 295 K Cu array. Inset shows the configuration of a two-element overlapping array; voxel-body surface and body-array distances were $z_p=2$ mm and $z_v=7$ mm, respectively.

$$R_{\text{tot}} = \sum_{j=1}^{N}\sum_{i=1}^{N} \alpha_i[(\beta R_{c_i} + \gamma R_{e_i})\delta_{i,j} + R_{b_{i,j}}]\alpha_j^*. \quad (5)$$

R_{tot} is defined here to include a weighted sum of the noise from each coil. The weighting coefficients α_i selected above are the same as those derived for the signals. Matrices R_{c_i} and R_{e_i} represent coil and electronics circuitry noise resistance at room temperature T_{RT} in each channel, respectively. $R_{b_{ij}}$ represents a body noise resistance component associated with the jth coil and seen by the ith coil.[7] β and γ are the noise reduction factors $\beta=(T/T_{\text{RT}})[R_s(T)/R_s(T_{\text{RT}})]$ and $\gamma=(T/T_{\text{RT}})[R_e(T)/R_e(T_{\text{RT}})]$ describing the influence of temperature (T) on the coil's surface resistance (R_s) and on electronics loss R_e. δ_{ij} is the Kronecker delta function.

Results of the relative SNR calculations for 77 K Cu and for HTS arrays are shown in Fig. 3. Each element was fully decoupled from adjacent elements by the geometrical overlapping method. The number of elements equal to one indicates a one-element (25×50 mm^2) "array," whereas eight elements represents a configuration of eight 8×25 mm^2 coils in an array.

Both coils were tested as an array by acquiring in the 4.7 T Bruker scanner moderately T_2-weighted axial slices of tumors present in a mouse. The inset in Fig. 4 shows such an image when each animal was placed under an element of the array and both FOV were acquired simultaneously.

In MRI the SNR is defined as an SNR root-mean-square voltage ratio, so 6 dB is equivalent to 100% gain. The SNR of an array is approximately equivalent at least to the SNR of a single element in this array.[15] The simulations presented in Fig. 3 show very significant gains over 295 K Cu array ($\sim$6 and $\sim$11 dB) for $N=2$. Such gains were confirmed by measuring SNR maps of each individual element of three identically designed coil arrays (Fig. 4) where, for small array-body distance, the SNR gain of HTS coil over Cu 295 K coil at depth of 7 mm is close to 12 dB. In theory, SNR gain should not be dependent on distance from the coil; however, in our experiment small differences between effective coil sizes and in coil-body configuration introduced such dependence. Also obtained smaller than expected gain of the 77 K Cu coil is caused by higher electronics loss for the Cu coil.

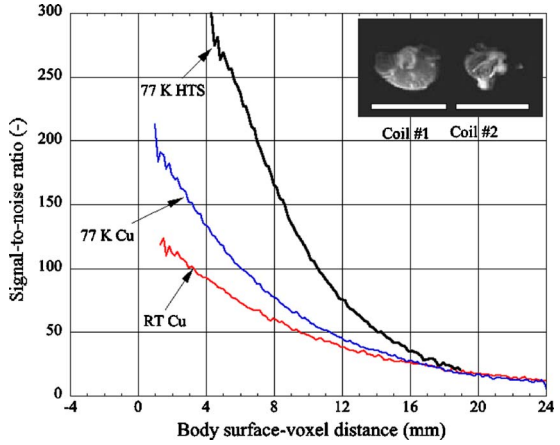

FIG. 4. (Color online) Plots of experimentally measured SNR vs distance z_v between a body surface and voxel for an individual element of 295 K Cu, 77 K Cu, and 77 K HTS arrays. SNR was calculated as a ratio of the image pixel value to standard deviation of pixel values outside the image area. Inset shows an image of two mice put side by side and acquired by both elements (24 mm in diameter each) working at the same time (as an array).

The HTS coil had electronics cooled whereas the 77 K Cu coil was measured with electronics kept at room temperature.

Today, due to the development of new signal processing techniques, virtually all receiving coils used in clinical MRI are designed as arrays. The trend is to further increase the number of arrays elements thus to reduce the size of the receive coils. Therefore, HTS arrays in light of these developments and trends should become indispensable for further SNR improvement.

The two-coil design presented here can be extended to a larger number of elements either in linear or square shape arrays.[16] A double-sided structure of each coil [see Fig. 1(a)] allows for design flexibility with different schemes of both coupling and decoupling capacitors.[13] In addition, if such HTS array is used alongside time reduction techniques, imaging time will be reduced by a factor of 2 while still preserving very high SNR value of the HTS coils.

[1] M. T. Vlaardingerbroek and J. A. den Boer, *Magnetic Resonance Imaging*, 3rd (Springer, Berlin, 2003), 244.
[2] P. Styles and N. F. Soffe, J. Magn. Reson. (1969-1992) **60**, 397 (1984).
[3] R. S. Whithers, G.-C. Liang, B. F. Cole, and M. Johansson, IEEE Trans. Appl. Supercond. **1**, 2450 (1992).
[4] J. G. van Heteren, T. W. James, and L. C. Bourne, Magn. Reson. Med. **32**, 396 (1994).
[5] R. D. Black, T. Early, P. Roemer, O. Mueller, A. Mogro-Campero, L. Turner, and G. Johnson, Science **259**, 793 (1993).
[6] L. Darrasse and L. C. Ginefri, Biochimie **85**, 915 (2003).
[7] P. B. Roemer, W. A. Eldelstein, S. P. Souza, C. E. Hayes, and O. M. Mueller, Magn. Reson. Med. **16**, 181 (1990).
[8] K. P. Prussman, M. Weigner, M. B. Scheidegger, and P. Boesiger, Magn. Reson. Med. **42**, 952 (1999).
[9] Z. Y. Shen, *High-Temperature Superconducting Microwave Circuits* (Artech House Antennas and Propagation Library, MA, 1994), 231.
[10] J. Wosik, L.-M. Xie, K. Nesteruk, L. Xue, M. R. Kamel, J. A. Bankson, and J. D. Hazle, IEEE Trans. Appl. Supercond. **13**, 1050 (2003).
[11] P. Gonord and S. Kan, Rev. Sci. Instrum. **65**, 509 (1994).
[12] Theva Dünnschichttechnik GmbH, Germany.
[13] U.S. Patent Application No. 2007/0013377A1 (pending).
[14] P. Hoult and R. E. Richards, J. Mater. Res. **24**, 71 (1976).
[15] S. M. Wright and L. L. Wald, NMR Biomed. **10**, 394 (1997).
[16] J. Wosik, K. Nesteruk, K. R. Kamel, L. Xue, L-M. Xie, K. H.Bockhorst, and P. A. Narayana, *Proceedings of the 14th Annual Meeting of the International Society of Magnetic Resonance in Medicine* (Mira Digital Publishing, Seattle, WA, 2006), Vol. 14, p. 527.